HOW HAVE ØRSTED, CHAMP, AND SAC-C IMPROVED OUR KNOWLEDGE OF THE OCEANIC REGIONS

M. Purucker [1], T. Sabaka [1] , N. Olsen [2], and S. Maus [3]

[1] Raytheon ITSS at Geodynamics Branch
Goddard Space Flight Center, Greenbelt, MD 20771, USA,
Email: purucker@geomag.gsfc.nasa.gov, sabaka@geomag.gsfc.nasa.gov
[2] Danish Space Research Institute, Copenhagen, Denmark, Email: nio@dsri.dk
[3] GeoForschungsZentrum, Potsdam, Germany, Email: smaus@gfz-potsdam.de

ABSTRACT

This talk presents an overview of the capabilities and accomplishments of the current generation of magnetic field satellites, especially with respect to improvements in the oceanic region. Two types of improvements are discussed: 1) in our ability to continuously monitor secular variation in the oceanic regions, and 2) in the characterization of the anomalous vector field associated with lithospheric magnetization. Improvements seen in the lithospheric field include both the ability to resolve subtle features, like the enhanced magnetization associated with spreading zones, and the ability to improve our knowledge of isochron location in poorly surveyed parts of the ocean.

INTRODUCTION

In this brief survey, we'd like to provide an overview of the following topics: 1) secular variation over the North Atlantic Ocean from 1980 to the present, 2) oceanic vs. continental magnetic fields, and 3) observations vs. predictions for the North Atlantic and Pacific Oceans.

SECULAR VARIATION

The earth's magnetic field is constantly changing. On the continents we monitor this change with magnetic observatories. This is currently almost impossible to do on the oceans (although sea-bottom observatories may change that) and so satellites are our best source of secular variation information over the oceans. Prior to Ørsted, CHAMP, and SAC-C our knowledge of secular variation of the vector magnetic field from satellites was limited to the Magsat mission, from which it was difficult to extract secular variation because of its short, 6-month, lifetime. So we've entered a new age of being able to continuously monitor global secular variation, our only direct measure of motion in the fluid outer core, even over the oceans. As an example of our capability, we show, in Figure 1 (upper left), the accumulated secular variation in the total field over the western Atlantic Ocean between the Magsat mission and the early days of Ørsted. Notice that the decrease in this region amounts to some 5% of the total field, a significant figure. We can compare that secular variation with that measured from Ørsted between 2000.0 and 2001.0 and based on a co-estimated main field and secular variation model, using a color scale that is scaled to the color scale for the 1980 to 2000 time frame (Figure 1, lower left). We can see that the area of maximum field decrease is reduced in size. Finally, we can utilize actual satellite profiles (their locations are shown in red on the lower left in Figure 1) from the SAC-C satellite to show the continuation of that secular decrease for a 13 month period beginning in February of 2001. The observations here have been selected from magnetically quiet times (the Dst index, a measure of the ring current, is between 0 and +10 nT) at 22:00 LT and reduced using a main field for 2001.0 Advances in the characterization of secular variation are continuing, and two of the goals are to characterize short term phenomena such as oscillations of the core and geomagnetic jerks.

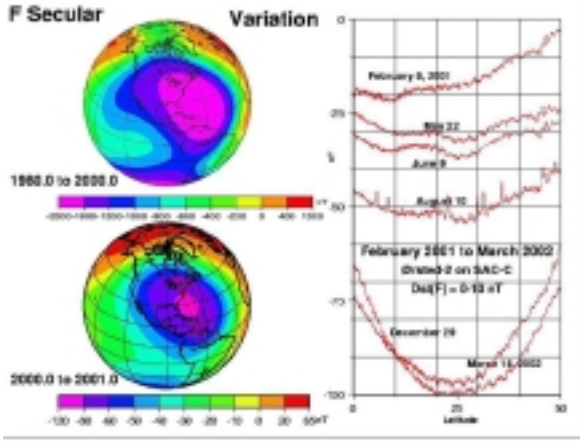

Figure 1: Oceanic secular variation

SATELLITE OBSERVATIONS REDUCED TO MODEL

In order to evaluate how Ørsted, CHAMP, and SAC-C have improved our knowledge of the oceanic lithosphere, we compare what we consider to be the best model made from earlier data and techniques (the M102389 model based on Magsat, shown in the left hand column of Table 1) with three models produced (or published) this year (shown in the right hand columns of Table 1). We will subsequently refer to these in shorthand as the observations, in order to contrast them with

predictive lithospheric models based on non-satellite data, to be discussed next. The properties of these observations are summarized in Table 1.

	M102389	IDEMM	CM3e:A	MF1
Satellites	Magsat	Orsted & CHAMP	POGO,Magsat, Orsted,CHAMP	CHAMP
Static Degree	49	49	65	80
Degrees Used	15-40	15-44	15-58	15-80
Scalar-Vector	25%-75%	Scalar poleward of 48 geomag lat.	Scalar & vector	Scalar only
Observatory	As slope	As slope	As field, Solves for bias	None
Secular Variation Degree	10	16	13	N.A.
Ionosphere	Correction only	Non-auroral area selection	QD, 1-D Ind., Resolves EE	22:00 to 06:00 LT only
Magnetosphere	From Dst	Degree 2 w Dst	Dst, 1-D Ind.	3-parameter fit for each pass
Coupling Currents, Induction	None	None	Radial currents, 1-D induction	None
Reference	Cain, 1990	Olsen, 2002	Sabaka & Olsen, 2002	Maus et al, 2002

Table 1: Observations reduced to models

PREDICTIVE LITHOSPHERIC MODELS

The Ørsted era has seen the development of predictive models (Table 2) of induced and remanent magnetization in the oceanic and continental lithosphere. These models capture the longest wavelength features of the Cretaceous Quiet Zones, and the continent-ocean magnetization contrast that overlaps with the core field. Some of these fields are unresolvable but they have important consequences for interpretation. For example, Purucker et al. (2002) have recently shown that the large, total-field anomalies centered over Kentucky, USA, and the south-central USA could be the manifestations of the magnetic edges of the southern boundaries of cratonic North America. On other continents, where our knowledge of the deep lithosphere is not as complete, these models still need improvement but at the same time offer the promise of a better understanding of the lithosphere if we can deconvolve the observations. A similar pattern holds over the oceans, as we will see next.

	3SMAC+DAH
Induced Model	Volume of magnetic crust and its magnetic susceptibility
	3SMAC model used for crustal thickness & temperature Reduced using sediment thickness model
	Assumed magnetic susceptibility = 0.04 SI (Oceans) = 0.035 SI (Continents)
Remanent Model	Restricted to oceanic lithosphere. Based on non-satellite input calibrated with Magsat (M102389) in S.Atlantic
	Magnetization vector intensity & direction based on ocean floor ages, and motion model for each plate
	Oceanic micro-continents, plateaus, and subduction zones not included in model
References	Purucker, Langlais, Olsen, Hulot,Munden, GRL, 2002 Dyment & Arkani-Hamed, 1998, JGR (DAH) Natuf & Ricard, 1996, PEPI (3SMAC)

TABLE 2: PREDICTIVE MAGNETIZATION MODEL

We illustrate in Figure 2 how the model is constructed using an example from the North Atlantic Ocean. We begin in the lower left (Figure 2) with the induced model, which is based on the volume of the magnetic crust and its magnetic susceptibility. Shown is the lithospheric field in the direction of the main field (total field anomaly). The negative total field values in the oceanic region flanking Greenland reflect the contrast in magnetic crustal thickness between Greenland and the surrounding oceans. Notice the presence of very long wavelengths, including those not observable because of overlap with the core field. Those unresolvable wavelengths will be removed in the final step. The remanent model is shown in the lower right (Figure 2) and is dominated by the long-wavelength content of the Cretaceous Quiet Zones, and by new, relatively magnetic crust, in the Davis strait separating Greenland and Canada. Notice that the field in the northern Davis strait is opposite to that predicted by the induced model, and hence there will be some cancellation of fields. The sum of the induced and remanent model is shown in the upper left (Figure 2). Finally, we restrict the spatial content of the model to those that can actually be

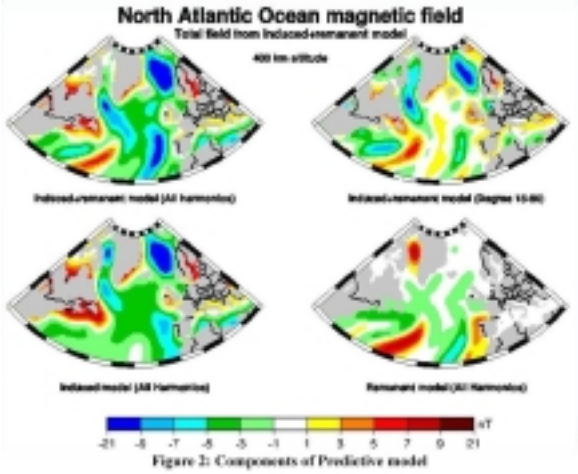

Figure 2: Components of Predictive model

observed by the satellites, from degrees 15 through 80 or so (Figure 2, upper right).

OCEANIC VS CONTINENTAL MAGNETIC FIELDS

The oceanic and continental crust differ in many ways. As a consequence we might expect there to be a difference in magnetic signature. For example, they typically differ by a factor of 5 in their thickness. Because what is sensed at satellite altitude is the product of the magnetization or susceptibility times the magnetic thickness, a factor of 5 difference in thickness will translate to a factor of 5 difference in magnetic field intensity for comparable magnetization or susceptibilities. Partially counter-balancing the increased thickness of the continents is the strength of magnetization in the oceans, for example within the extrusive basaltic layer, especially near the ridge axis.

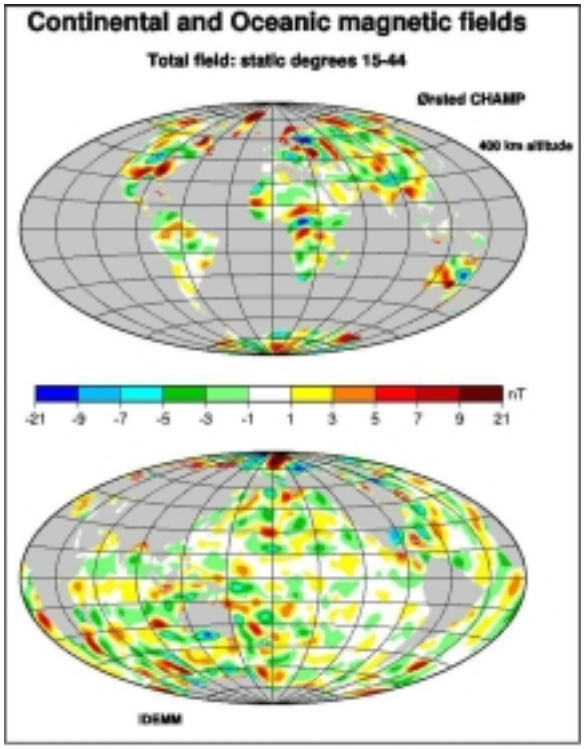

Figure 3: Oersted/CHAMP fields

In this representation (Figure 3) of the latest observations from Ørsted and CHAMP, we have masked the oceans in the top figure in order to highlight the continental magnetizations. Note that the continents contain the largest (Kursk and Bangui) anomalies. In the lower figure, we have masked the continents and show the oceanic magnetic fields, again from the Ørsted and CHAMP observations. Notice that some of the strongest anomalies are near the continental edges (for example in the Gulf of Mexico, south of Australia, and southeast of Australia). These have been interpreted as part of the signature of the continent-ocean contrast (Gulf of Mexico and south of Australia) or of submerged micro-continents (Lord Howe Rise). Notice also that much of the Pacific Ocean is characterized by weak magnetic fields.

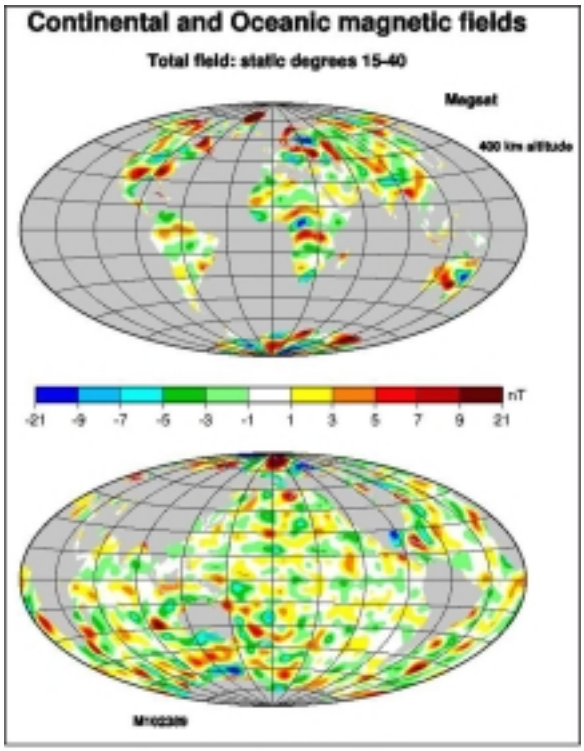

Figure 4: Magsat fields

In the map (Figure 4) made using the earlier Magsat observations, note the similarity in both the strength and location of individual continental anomalies. Note also the increased magnetic field over the Pacific, and Indian Ocean regions. We interpret this feature to result from improvements in modeling the low- and mid-latitude external fields, and not to any secular change in the lithospheric field over the oceans.

NORTH ATLANTIC OBSERVATIONS AND PREDICTIONS

The magnetic anomaly field seen by CHAMP, through degree 80, is shown in Figure 5. We have masked the continents, and show only the oceanic magnetic fields. Oceanic spreading isochrons are shown with red lines, and fracture zones with black lines. As we'll see, the North Atlantic magnetic signatures are dominated by the Cretaceous Quiet Zone and the continent-ocean contrast.

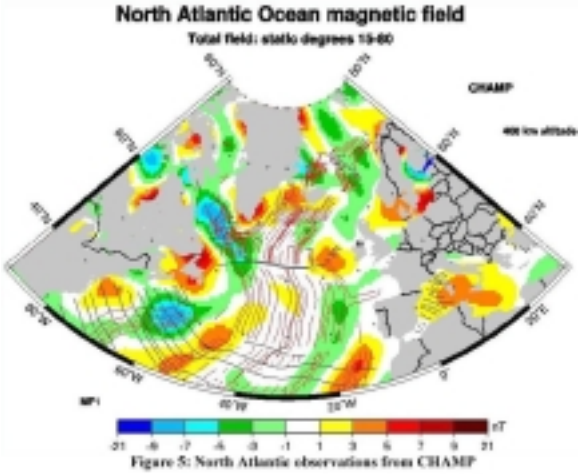

Figure 5: North Atlantic observations from CHAMP

Shown in Figure 6 are all four sets of satellite observations, with the oldest, and lowest resolution views of Magsat in the lower right. Ørsted and CHAMP data go into making the map at the lower right, CHAMP data alone go into making the map at the upper right, and POGO, Magsat, Ørsted, and CHAMP go into the map at the upper left. Notice that, with the exception of the anomaly marked 'A' on the Magsat map, the anomalies are very similar on all four maps. In the case of 'A', the positive anomaly is much reduced on the later Ørsted and CHAMP maps, and the region to the south of 'A' is dominated by a prong of positive magnetic field in the Ørsted and CHAMP maps, and by a region of negative magnetic field on the Magsat map.

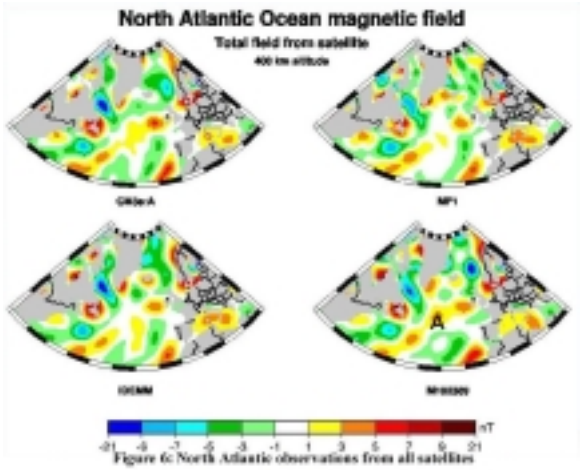

Figure 6: North Atlantic observations from all satellites

The comparison of the earlier Magsat observation (Figure 7, top left) with the prediction made from the global induced plus remanent model (Figure 7, top right) shows that the predictive model agrees more closely with the later Ørsted and CHAMP observations in the vicinity of 'A'. It also allows us a better understanding of the difference, which is related to a failure to isolate the signature from the more intensely magnetized mid-ocean ridge in this region. A more intensely magnetized mid-ocean ridge is predicted from most in-situ observations but it is a subtle feature and often difficult to observe in the satellite maps.

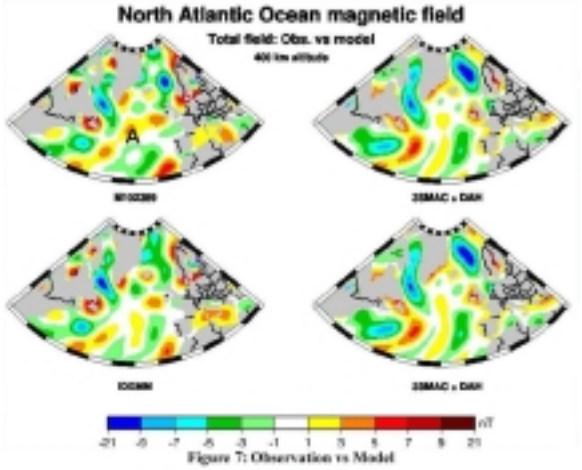

Figure 7: Observation vs Model

Notice that while the magnetic signature of the mid-ocean ridge is also observed in the Ørsted and CHAMP observations shown in Figure 8, it is not as large as predicted. This is seen in other regions, and in fact some ridges, like the East Pacific rise, still have no recognizable magnetic signature from satellite.

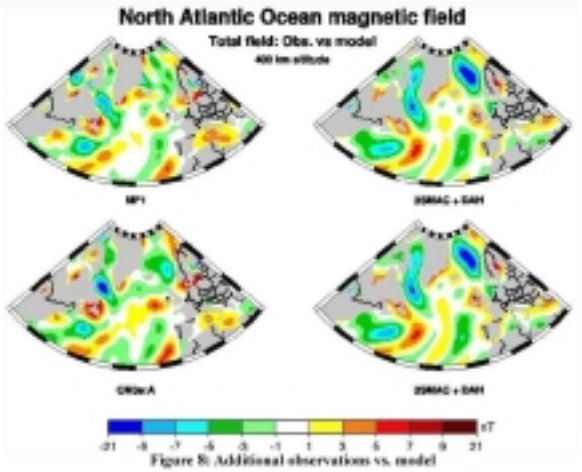

Figure 8: Additional observations vs. model

EQUATORIAL PACIFIC OBSERVATIONS AND PREDICTIONS

In Figure 9, the predicted field in the equatorial Pacific is shown in the upper right, along with the separate induced and remanent components that go into its construction. Notice that we are showing the radial field now instead of the total field which we showed on the previous maps of the North Atlantic. This is because the radial field is especially good at resolving features near the magnetic equator. Notice especially the predicted boundaries of the Cretaceous Quiet Zone in the western Pacific. They are shown in the upper right figure as anomalies B, C, and D and represent only the observable wavelength range of the much larger feature seen in red in the figures on the left hand side of Figure 9. It is much more difficult to observe the radial anomaly field than the total field, especially at the equator, and Ørsted and CHAMP have made significant improvements in this respect over Magsat.

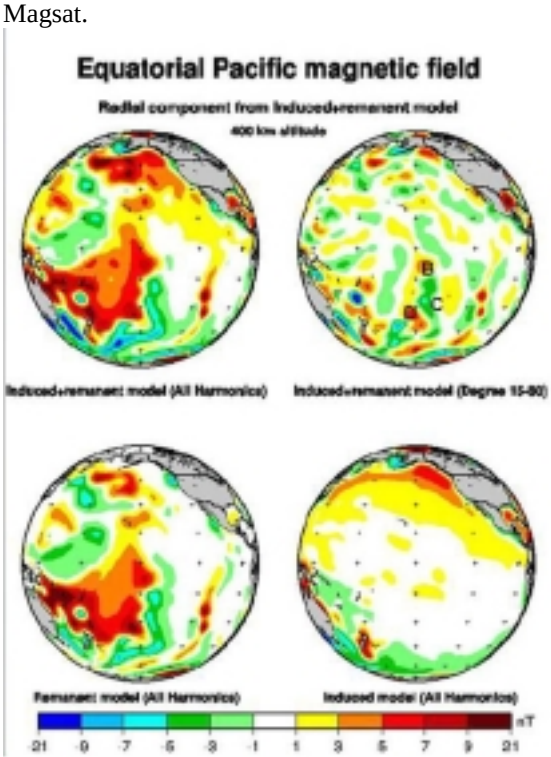

Figure 9: Equatorial Pacific model

In the observations (Figure 10), the northernmost 'B' anomaly is resolved in the older Magsat map, although the more southerly 'C' and 'D' anomalies are not. In contrast, they are resolved in all three of the current maps.

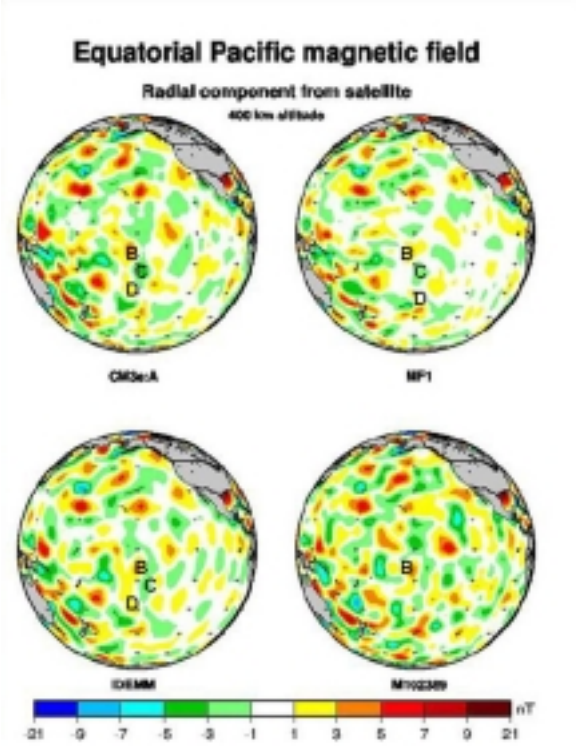

Figure 10: Observations

Let's now look at the expected vs observed location of these features (Figure 11). The edges of the Cretaceous Quiet Zone are systematically east of their predicted locations on the Ørsted and CHAMP map, shown on the bottom of Figure 11, with the largest offset at 'B' and the smallest at 'C'. This pattern is also found on the other recent maps, and is also true of the 'B' anomaly observed on the Magsat map, shown at the top of Figure 11.

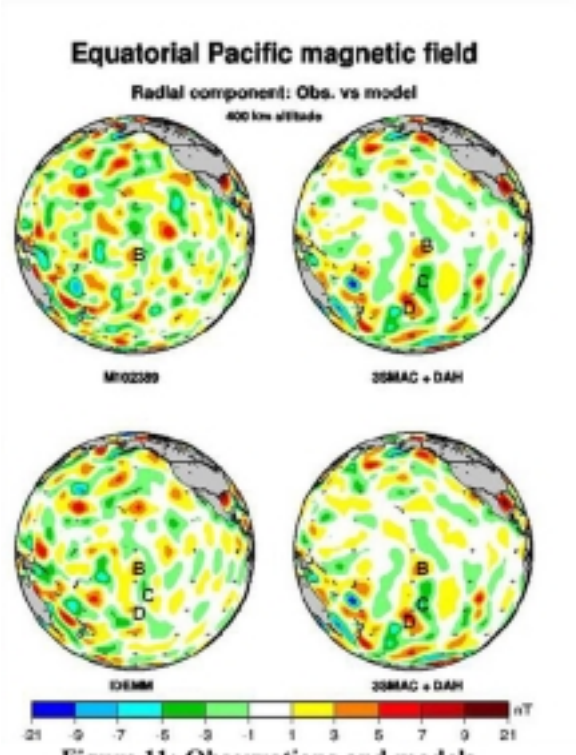

Figure 11: Observations and models

Figures 12a and b show the observed and predicted maps, respectively, and a comparison of them provides a feel of the offset. Remember, the black lines on the map are the fracture zones and the red lines are the seafloor spreading isochrons. In the case of 'B', the offset amounts to some 700 km in this poorly mapped region of the Pacific. The next step is to adjust, probably with several iterations, the locations of the isochrons in the underlying age map and follow the resulting changes. Additionally it will be important to better understand the constraints from the sparse marine surveys (NGDC, 1999) in the vicinity of the Galapagos, Marquesas, and Austral (from north to south) fracture zones. Finally, we need to explore the long-wavelength cutoff to ensure that we have not retained any signals of core origin. This may be especially important in regions where the lithospheric signal is weak, as in the oceans.

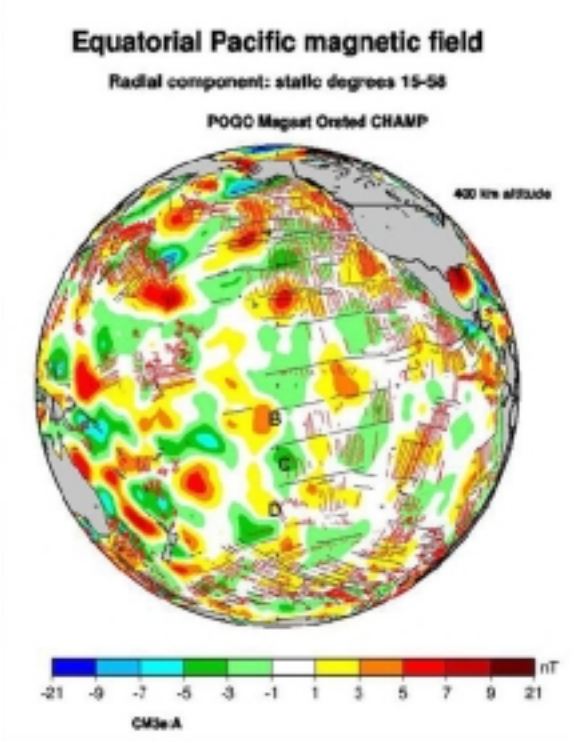

Figure 12a: Observations

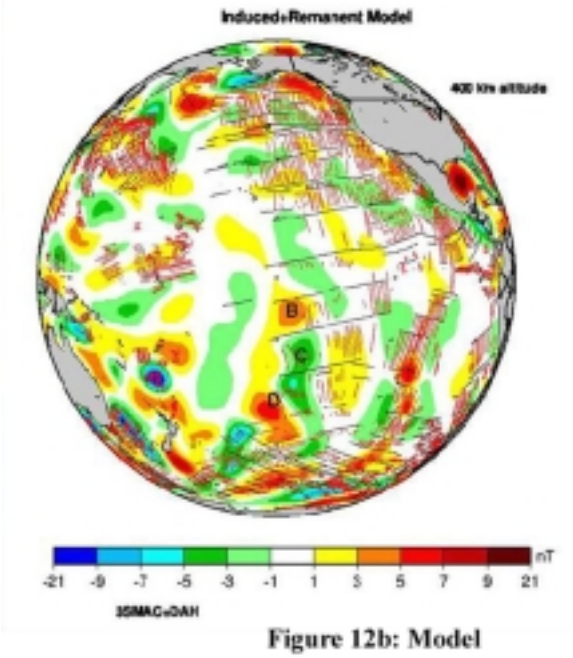

Figure 12b: Model

SUMMARY

We draw the following conclusions from an examination of Ørsted, CHAMP and SAC-C data and supporting models: 1) satellites can now confidently track secular variation, 2) the magnetic field amplitudes from our best models still vary significantly, but based on model improvements, we seem to be converging, 3) the first global models capable of predicting induced and remanent magnetic fields over the continents and oceans now exist. 4) the North Atlantic Ocean is well-characterized by the model of induced and remanent magnetization. Our best observations reduced to a model now resolve the mid-ocean ridge between 32 and 40 degrees North, and 5) in the Pacific Ocean there is tentative, tantalizing evidence to provide the first ever identification of the southeast edge of the Cretaceous Quiet Zone, and to suggest modifications to that poorly determined boundary.

ACKNOWLEDGEMENT

This paper is dedicated to the memory of Robert A. Langel and Stephen Zatman. Stephen had planned to attend this meeting, and to discuss his latest insights into torsional oscillations of the fluid core using observations such as these. He had done a postdoc in our group and had just begun a profesorial appointment in geophysics at Washington University when he was killed in an auto crash. He will be remembered for his outgoing ways and wit.

REFERENCES

Cain, J., Holter, B. and Sandee, D., (1990): Numerical experiments in geomagnetic modeling, *J. Geomag. Geoelec.*, Vol. 42, pp. 973-987.

Dyment, J. and Arkani-Hamed, (1998): Contribution of lithospheric remanent magnetization to satellite magnetic anomalies over the world's oceans, *J. Geophys. Res., Vol 103*, pp. 15423-15441.

Maus, S., Rother, M., Holme, R., Luehr, H., Olsen, N. and Haak. V., (2002): First scalar magnetic anomaly map from CHAMP satellite data indicates weak lithospheric field, *Geophys. Res. Lett.*, Vol. 29, 10.1029/2001GL013685.

National Geophysical Data Center, (1999): Marine trackline geophysics, 3 CDs.

Nataf, H. and Ricard, Y. (1996): 3SMAC: An a priori tomographic model of the upper mantle based on geophysical modeling, *Phys. Earth Plan. Int.*, Vol. 95, pp. 101-122.

Olsen, N., Holme, R., and Luehr, H., (2002): A magnetic field model derived from from Ørsted, CHAMP, and Ørsted-2/ SAC-C observations, *EOS Trans. AGU*, Vol 83(19), Spring Meeting Suppl., Abstract GP21A-01 and EOS, Vol. 83 (34), p. 368.

Purucker,, M. Langlais, B., Olsen, N., Hulot, G., and Mandea, M., (2002): The southern edge of cratonic North America: Evidence from new satellite magnetometer observations, *Geophys. Res. Lett.*, Vol 29, 10.1029/2001GL013645

Sabaka, T., Olsen, N., and R. Langel, (2002): A comprehensive model of the quiet-time, near-Earth, magnetic field: Phase 3, *Geophys. J. Int.*, Vol. 151, pp. 32-68.